

ADSORPTION - DESORPTION SYSTEM FOR CO₂ REMOVAL IN BIOGAS USING NATURAL ZEOLITE - BASED ADSORBENT

IRVAN^{1,2,*}, BAMBANG TRISAKTI^{1,2}, SERI MAULINA^{1,2},
RIVALDI SIDABUTAR¹, IRIANY¹, MOHD SOBRI TAKRIFF³

¹Department of Chemical Engineering, Faculty of Engineering, Universitas Sumatera Utara, Medan, 20155, Indonesia

²Sustainable Energy and Biomaterial Center of Excellence, Universitas Sumatera Utara, Medan, 20155, Indonesia

³Research Center for Sustainable Process Technology, Faculty of Engineering and Built Environment, Universiti Kebangsaan Malaysia, UKM, Bangi, Selangor DE, Malaysia

*Corresponding Author: irvan@usu.ac.id

Abstract

This study aimed to remove CO₂ from air-CO₂ mixture using natural zeolite-based adsorbent pellets through adsorption and to regenerate the adsorbents using air through desorption. The experiment was conducted to determine the percentage of CO₂ removal and breakthrough curve characteristics by varying the flow rate of the air-CO₂ mixture and the type of adsorbent pellet. The residual CO₂ content of purified gas was analysed every minute and stored in the gas collector. Pure air with ambient temperature ranging from 30 to 40 °C flowed through a column for desorption of CO₂ in the saturated pellet adsorbent. Results concluded that the best percentage of CO₂ removal was 92.5% by using adsorbent pellet with particle size of 140 mesh, calcination temperature 400 °C for four hours and a flow rate of mixed gas at 200 ml/min. This characteristic also described the optimum CO₂ desorption that is achieved at 40 °C of air temperature and flow rate of 200 ml/min for 20 minutes. The adsorption equilibrium was fitted using Langmuir isotherm with R² correlation value of 0.9962. Modelling of adsorption kinetics to describe breakthrough curve used pseudo-order and Elovich kinetics. The results showed that the pseudo-order kinetics provided good results under operating conditions.

Keywords: Adsorption, Biogas, Carbon dioxide, Desorption, Zeolite.

1. Introduction

In 2016, palm oil production in Indonesia reached 35 million tons obtained from 10.8 million hectares of plantations [1, 2]. Every ton of crude palm oil produces 2.5 tons of palm oil mill effluent (POME). In 2015, Indonesia produced 79.2 million tons or equivalent to 89.7 million m³ of POME [3]. If 1 m³ of POME can generate 28 m³ of biogas [4], then this country can produce 2511.6 million m³ of biogas, wherein 1 m³ of biogas can generate 2 kWh of power with the total the power potential of 5.02 billion kWh per year [5].

One of the problems in converting biogas from POME is the undesirable high CO₂ content in biogas. Biogas consists of 55%–70% CH₄, 30%–45% CO₂ and other components in small quantities, such as H₂S (1000 ppm–3000 ppm), NH₃ (80 ppm–100 ppm) and hydrocarbons (< 100 ppm) [6]. Every 15 m³ biogas with 35% CO₂ can produce 98 kWh of energy, whereas 13 m³ biogas with 5% CO₂ can generate 125 kWh of energy [7]. Reducing CO₂ levels in biogas increases the calorific value to produce energy.

Techniques in removing CO₂ from biogas include chemical and physical adsorption, pressure swing adsorption, cryogenic separation, membrane separation, biological–chemical CO₂ fixation and absorption [8, 9]. This research focused on applying adsorption for CO₂ removal. A material with large surface area and highly selective adsorption capacity [10] can be used as an ideal adsorbent for CO₂ removal. One of the dense adsorbents that can purify biogas is zeolite. In Indonesia, natural zeolite deposit is abundant, and its purity is high enough with silica content of 60%. Activated and modified natural zeolite can be used as the adsorbent for biogas [11]. The structure of zeolite can be used for adsorption of H₂O, CO₂, SO₂ and H₂S contents, but it does not adsorb CH₄ [12]. The adsorption ability of zeolite for these gases is up to 25% [13]. This study aimed to remove CO₂ from air-CO₂ mixture using natural zeolite-based adsorbent pellets through adsorption. The CO₂ adsorbed by the adsorbents was removed using fresh air through desorption to regenerate the adsorbent, thus creating a continuous process.

The use of natural zeolite as an adsorbent to adsorb CO₂ has been previously studied. However, this research synthesized the natural zeolite-based adsorbents by firstly forming them into pellets and then calcining these materials. In addition, the natural zeolite-based adsorbent pellets were designed to remove the CO₂ content in the biogas produced from previous research [14]. The CO₂ content in biogas within range the 30%–40% was reduced to ≤ 10%.

2. Materials and Methods

2.1. Materials

Natural zeolite was used as an adsorbent pellet purchased from PT. Indah Sari Windu, West Java, Indonesia. In this study, biogas feeds were modelled using air and CO₂ mixtures with a content of CO₂ 35%–40% (v/v). Water (H₂O) was used as a supporting material and as a natural adhesive to form the zeolite particles into pellets.

2.2. Experimental setup

The experiments were conducted in Ecology Laboratory at the Chemical Engineering Department, Universitas Sumatera Utara. Figure 1 shows the laboratory scale of

adsorption column as a purifier. Adsorption was conducted in a column with internal diameter of 9.1 cm and height of 91 cm. The adsorbents were placed in a column that is 45 cm high. The column had a manometer and flow metre to measure the column pressure and air-CO₂ mixture flowrate, respectively. Supporting equipment includes air chamber, air supply, CO₂ tank and inline mixer. Inlet and outlet CO₂ concentration of the column was measured by SAZQ biogas analyser, which was manufactured by Beijing Shi'an Technology Instrument Ltd., China.

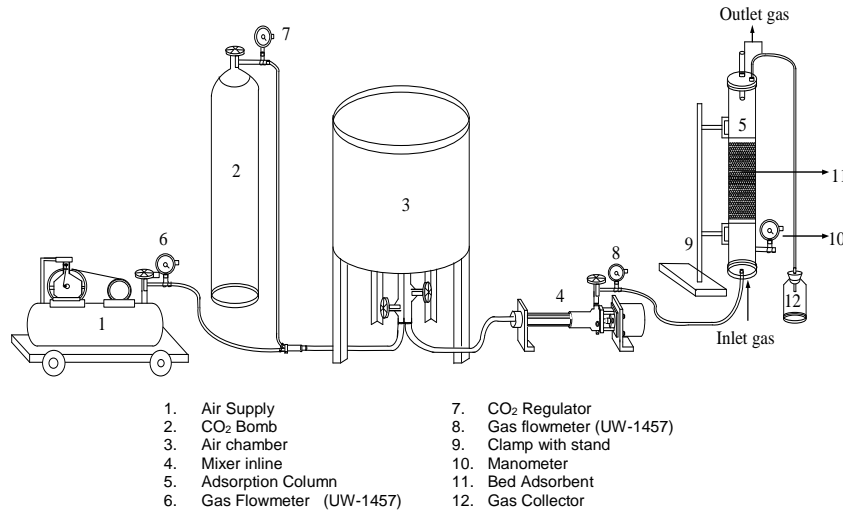


Fig. 1. Experimental set-up.

2.3. Methods

Adsorbents manufacturing

Adsorbents with various particle sizes and treatments were synthesized. The particle size variations were 50, 100 and 140 mesh, whereas the variations of temperature calcination were at 200 °C, 300 °C and 400 °C for 2, 3 and 4 hours, respectively. Table 1 summarises the type of all adsorbents manufactured in this research.

Table 1. The type of main adsorbent manufactured in this research.

No.	ϕ^*	T_c^{**}	t_c^{***}	No.	ϕ^*	T_c^{**}	t_c^{***}	No.	ϕ^*	T_c^{**}	t_c^{***}
1	140	400	4	10	140	200	4	19	50	400	4
2	140	400	3	11	140	200	3	20	50	400	3
3	140	300	4	12	140	200	2	21	50	400	2
4	100	400	4	13	100	400	2	22	50	300	4
5	100	400	3	14	100	300	3	23	50	300	3
6	100	300	4	15	100	300	2	24	50	300	2
7	140	400	2	16	100	200	4	25	50	200	4
8	140	300	3	17	100	200	3	26	50	200	3
9	140	300	2	18	100	200	2	27	50	200	2

* Particle sizes of natural zeolite (mesh)

** Calcination temperature (°C)

*** Calcination time (hours)

Adsorption

The adsorption was conducted by placing the adsorbents into the column. Air and CO₂ were mixed into the air chamber until a constant concentration of CO₂ of 40% (v/v) was achieved. The mixed gas was fed into an inline mixer to maximise the mixing. The flow rate of mixed gas varied at 200, 400 and 600 ml/min. The adsorption was performed for 30 minutes at pressure of 1 atm. The residual CO₂ content of purified gas was analysed every minute by SAZQ biogas analyser and stored in the gas collector. The collected data were used to determine CO₂ removal efficiency, breakthrough curve, equilibrium adsorption, adsorption kinetics and capacity and breakthrough time.

Desorption

For desorption, pure air was used as a carrier at an ambient temperature ranging from 30 °C to 40 °C. Adsorption–desorption experiment was conducted in series (consisted of three runs) by using the same type of adsorbent (type A) at the mixed gas flow rate 200 ml/min. Saturated adsorbent from the adsorption (Run 1) was regenerated through desorption at ambient temperature. This regenerated adsorbent was reused for Run 2 and then regenerated at 30 °C and then used for Run 3 and regenerated at 40 °C. The output air was analysed every minute by SAZQ biogas analyser until the CO₂ concentration was 0. The collected data were used to determine CO₂ removal efficiency and adsorption–desorption cycle time.

Langmuir adsorption equilibrium

Equation (1) [15] shows that the experimental data obtained were fitted by adsorption equilibrium of Langmuir.

$$\frac{C_e}{q_e} = \frac{1}{K_L q_m} + \frac{C_e}{q_m} \tag{1}$$

where q_m is the adsorption capacity (ml/g), K_L is the Langmuir equilibrium constant (ml/g), q_e is the amount of adsorbate per mass of adsorbent (ml/g) and C_e is the concentration of adsorbate at equilibrium.

Modelling of adsorption kinetics

The adsorption kinetics used in this study is pseudo-first order kinetics and Elovich kinetics. Equations (2) and (3) show the equations of pseudo-first order and Elovich, respectively [15].

$$\log(q_e - q_t) = \log q_e - \frac{K_1}{2.303} t \tag{2}$$

$$q_t = \frac{1}{\beta} \ln(\alpha\beta) + \frac{1}{\beta} \ln t \tag{3}$$

where q_t is the amount of adsorbate at time t (min), K_1 is the rate constant of the pseudo-first order (min⁻¹), q_e is the adsorption equilibrium capacity (ml/g) and α and β are the Elovich constants.

3. Results and Discussion

3.1. Effect of flow rate on percentage of CO₂ removal in air-CO₂ mixture

The percentage CO₂ removal was measured using the same type of adsorbent (140 mesh, 400 °C for 4 hours) and varying the flow rate of the air-CO₂ mixture at 200, 400 and 600 ml/min for 30 minutes. Figure 2 shows that the percentages of CO₂ removal at flow rates of 200, 400 and 600 ml/min were 92.5%, 82.5% and 60%, respectively. Therefore, if the flow rate is slow, then the percentage of CO₂ removal increases with the residence time. These results are consistent with those reported by Kesnawaty [16], who revealed that if the flow rate is low, then the contact time between gas-adsorbent in the adsorption column becomes long. Thus, the percentage of removal increases because the time is sufficient for the gas molecules to diffuse into the adsorbent pores [16]. Basu et al. [17] assumed that the mass transfer rates increase at high flow rates but lead to fast saturation. Conversely, the adsorption capacity decreased with the increase in flow rate because the residence time of adsorbate in the column was short.

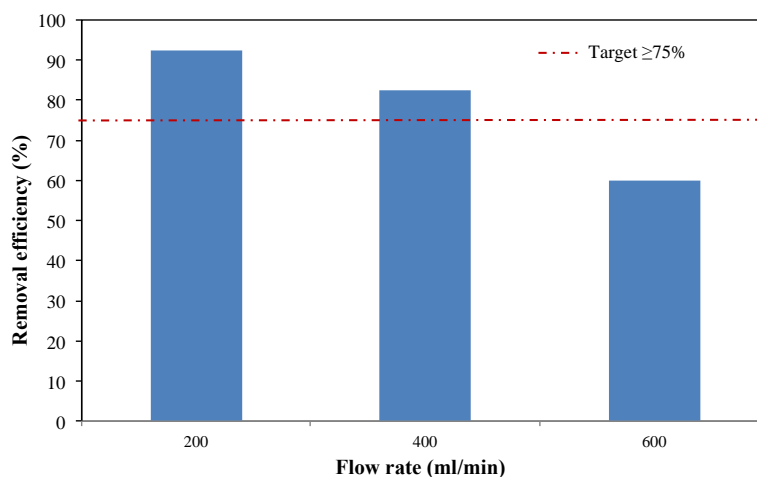


Fig. 2. Effect of mixed gas flow rate on the percentage of CO₂ removal.

3.2. Effect of pellet particle size on percentage of CO₂ removal in air-CO₂ mixture

The effectiveness of CO₂ removal must be evaluated by using different adsorbent particles to achieve a CO₂ removal target to determine the ability of zeolite as an adsorbent for CO₂ removal [13]. This research aimed to obtain adsorbent pellets that can reduce CO₂ content to $\pm 10\%$. The CO₂ content in biogas from POME is approximately 40%–60% [18]. The presence of CO₂ in biogas does not decrease the heating value, but most engines work optimally using biogas as fuel when the CO₂ content is below 10%. In Sweden, the components of CO₂, O₂ and N₂ in biogas should be below 5% by volume to allow usage as a vehicle fuel as requested by Swedish motor industry [19]. Table 2 shows the types of adsorbent, which can reduce CO₂ content below 10%. The acceptable CO₂ removal efficiency in this study was $\geq 75\%$. The pellet adsorbent with the lowest efficiency was type F with 75% efficiency.

Figure 3 presents the percentage of CO₂ removal from the air-CO₂ mixture for each type of adsorbent pellet with zeolite particle sizes of 50, 100 and 140 mesh at calcination temperature 400 °C. The figure shows that the 140-mesh adsorbent pellet could reduce CO₂ content with the highest removal efficiency compared with the 100- and 50-mesh pellets. This phenomenon occurred because the 140-mesh size has a larger surface area than the 50- and 100-mesh sizes. The adsorption capacity was determined by the surface area of the adsorbent. The amount of adsorption was proportional to its surface area. The smaller the particle size of the adsorbent, the larger the surface area and the greater the adsorption capacity [20].

Table 2. Types of adsorbent, which can reduce CO₂ content below 10%.

Adsorbent types	Initial CO ₂ concentration (% v/v)	Final CO ₂ concentration (% v/v)	Removal efficiency (%)
A	40	3	92.50
B	40	5	87.50
C	40	6	85.00
D	40	6	85.00
E	40	7	82.50
F	40	10	75.00

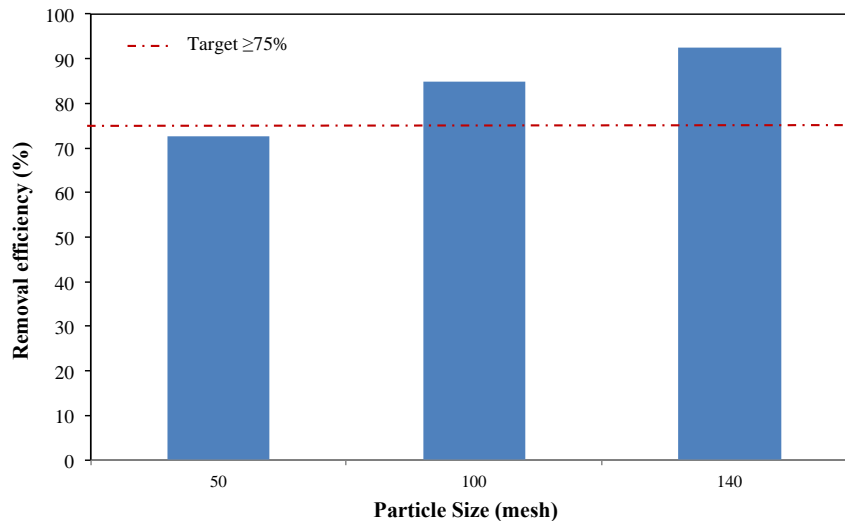


Fig. 3. Effect of pellet particle size on percentage of CO₂ removal.

3.3. Breakthrough curve

The breakthrough curve data of CO₂ removal must be obtained to determine the breakthrough time and adsorption capacity [16]. Figure 4 shows the breakthrough curve of CO₂ removal by various types of pellet adsorbent at the flow rate of 200 ml/min. From the breakthrough curve, the adsorption capacity can be seen. If the ratio value of initial and final CO₂ concentration approach to one ($C_t/C_o = 1$), then the adsorbent becomes saturated, and the adsorption becomes ineffective. If the breakthrough curve progressively moves to the right, then the adsorption saturates for a long time. A long breakthrough indicates great adsorption capacity. This experiment

aimed to obtain the adsorption capacity from six types of adsorbent at air-CO₂ mixture with flow rate of 200 ml/min. The optimum adsorbent type obtained was used again at different flow rates of at 400 and 600 ml/min. Figure 5 shows the effect of various pellet adsorbents on CO₂ adsorption capacity at flow rate of 200 ml/min. The highest adsorption capacity of 0.09236 mmol/g was achieved for particle pellet type A with the longest breakthrough time of 16.7 minutes.

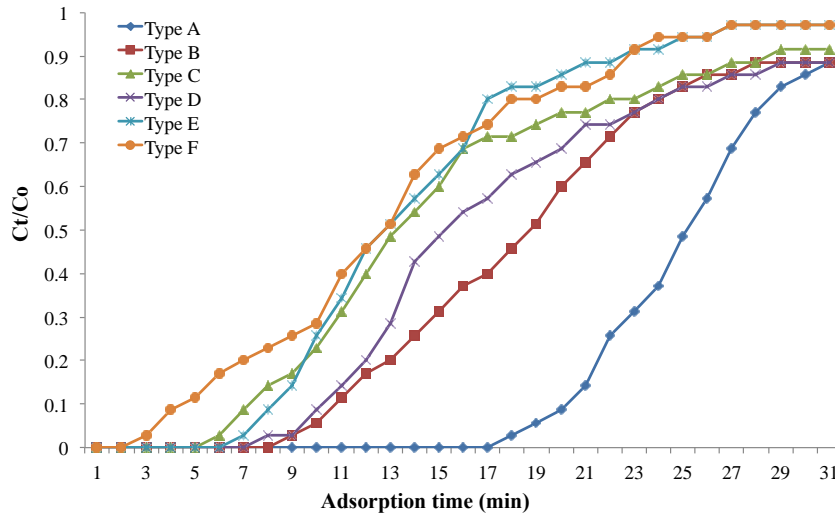


Fig. 4. Breakthrough curve of CO₂ removal in air-CO₂ mixture at flow rate 200 ml/min with various of adsorbent types.

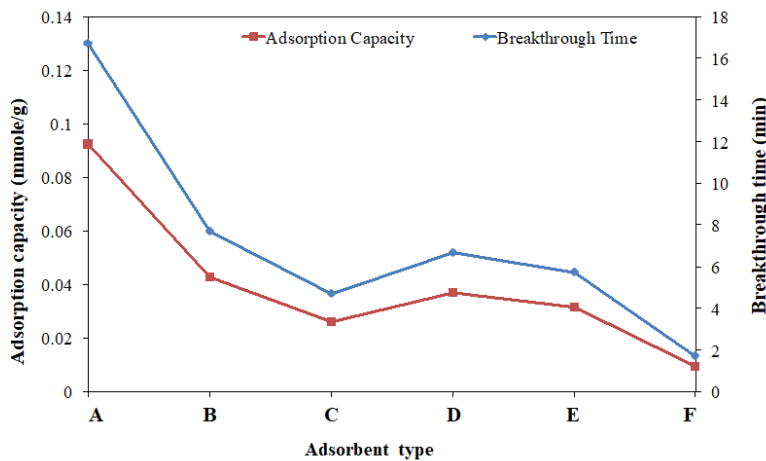


Fig. 5. Effect of adsorbent types on CO₂ adsorption capacity in air- CO₂ mixture at flow rate 200 ml/min.

Figure 6 shows the breakthrough curve of CO₂ removal by various air-CO₂ mixture flow rates using pellet particle of 140 mesh and calcination temperature of 400 °C for 4 hours (type A). Figure 7 shows the effect of flow rate on CO₂ adsorption capacity by using the same adsorbent. The highest adsorption capacity was achieved at flow rate of 400 ml/min with a breakthrough time of 10.7 minutes,

and the largest breakthrough adsorption capacity was 0.118 mmol/g. Therefore, if the breakthrough time becomes long and the flow rate becomes high, then the breakthrough adsorption capacity also increases. This result is consistent with those reported by Kesnawaty (2010), who stated that the value of adsorption capacity becomes small [16] when the breakthrough time is short. The greatest breakthrough time for all variations of air-CO₂ mixture flow rate and types of pellet adsorbent was achieved by the adsorbent type A and flow rate of 200 ml/min with a breakthrough time of 16.7 minutes. However, this result was relatively small, and the adsorption-desorption was frequently conducted.

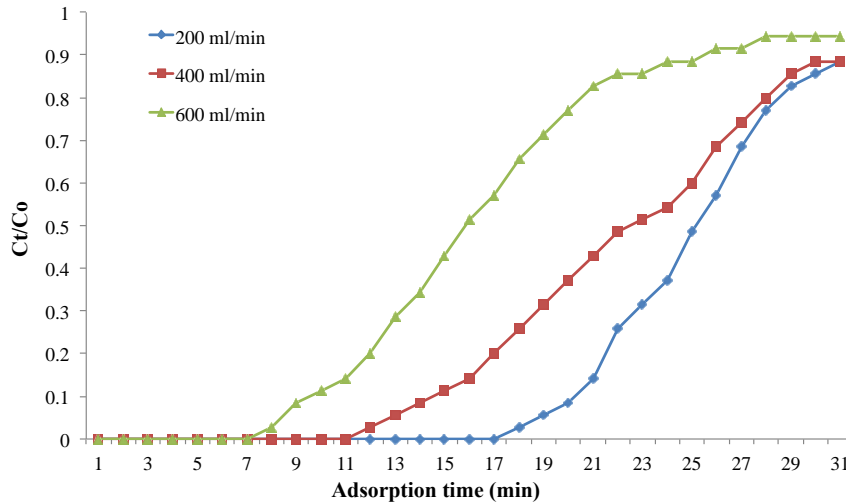


Fig. 6. Breakthrough curve of CO₂ removal using adsorbent type A at various of air-CO₂ mixture flow rate.

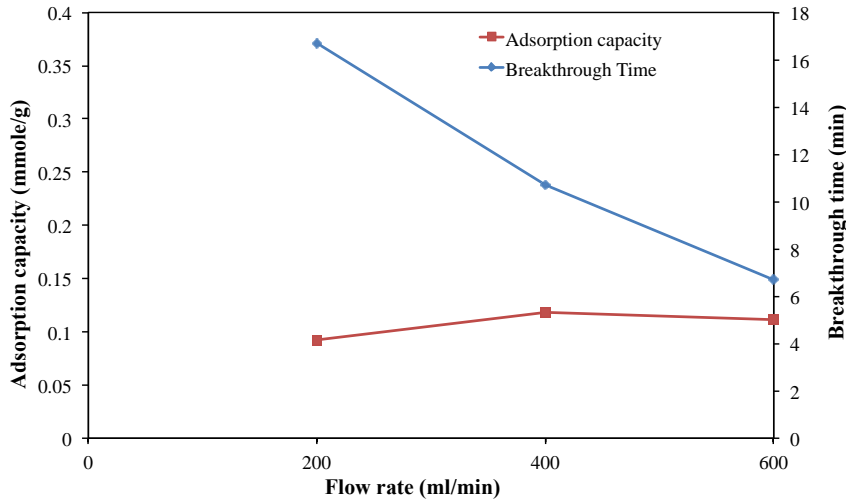


Fig. 7. Effect of flow rate on CO₂ adsorption capacity by using adsorbent type A.

3.4. Adsorption equilibrium

The kinetics data of CO₂ removal should be obtained to predict the ability of an adsorbent to adsorb a certain component [21]. Equation (1) [15] presents that the experimental data obtained were fitted by adsorption equilibrium of Langmuir.

CO₂ adsorption equilibrium was determined by plotting (C_e/q_e) versus (C_e). Figure 8 shows the curve (C_e/q_e) versus (C_e) on gas removal using adsorbent pellet type A at flow rate 200 ml/min. The curve formed a linear line with good conformance, where the results obtained the R² correlation of 0.9962 with Langmuir equation:

$$\frac{C_e}{q_e} = 0.109 + 2.082 C_e \quad (4)$$

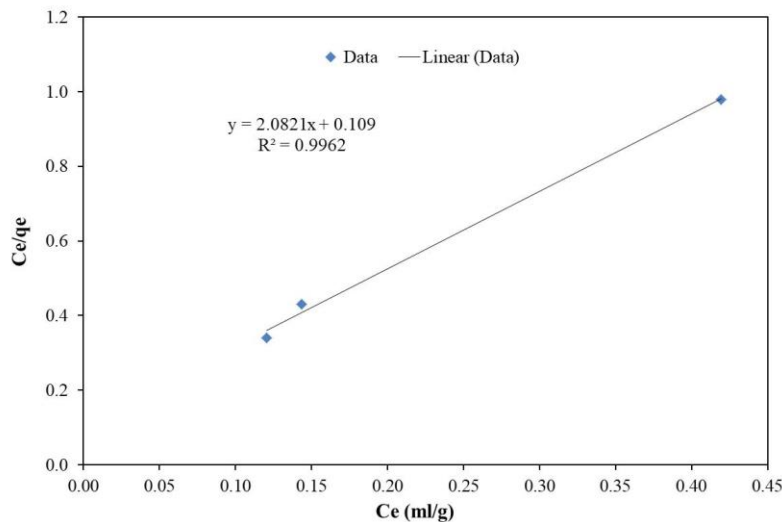


Fig. 8. Plot for Langmuir isotherm for the adsorption of CO₂.

3.5. Adsorption Kinetics

CO₂ adsorption kinetics was identified using various adsorbent types. The six types of adsorbent with the removal efficiency of $\geq 75\%$ determined the adsorption kinetics.

Pseudo-first order kinetics was verified by creating a slope and intercept of pseudo-first-order plots between $\log(q_e - q_t)$ versus t . Determining a kinetic model depends on the coefficient of determination (R^2). A suitable kinetic model must have an R^2 value that is high or close to 1 [22]. Elovich kinetic was verified from slope and intercept plots between qt versus $\ln t$. Figures 9 and 10 show the removal of CO₂ in air-CO₂ mixture using adsorbent type A at a flow rate of 200 ml/min.

These figures show that the R^2 value of Elovich kinetics is lower than that of the pseudo-first order kinetics. Therefore, the best and acceptable kinetic model is the pseudo-first order kinetic because it has a high R^2 value of 0.9848, indicating its suitability to serve as a kinetic model for CO₂ adsorption system on air-CO₂ mixture. Table 3 shows the kinetic parameters for CO₂ adsorption with various adsorbent types.

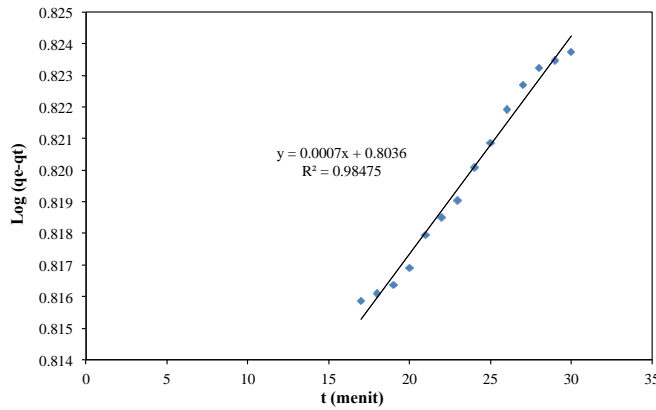


Fig. 9. Pseudo-first order kinetic plots for the adsorption of CO₂.

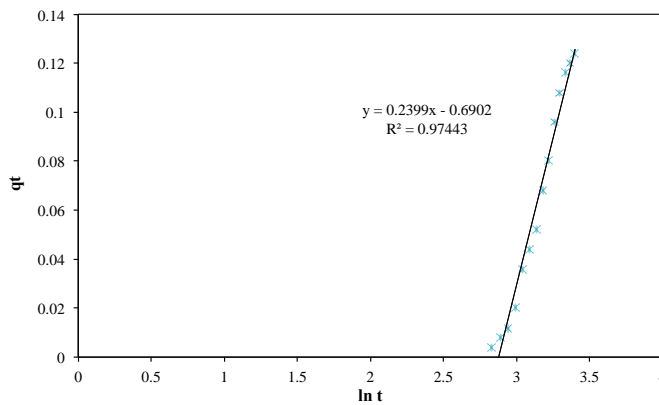


Fig. 10. Elovich kinetic plots for the adsorption of CO₂.

Table 3. Kinetic parameters for CO₂ adsorption at various adsorbent type.

Types	Pseudo-first order			Elovic		
	K_1 (min ⁻¹)	q_e (mg/g)	R^2	α	β	R^2
A	0.0016	6.362	0.984	4.168	0.501	0.974
B	0.0011	6.489	0.987	9.066	0.786	0.974
C	0.0009	6.534	0.904	12.610	0.877	0.975
D	0.0009	6.510	0.926	10.152	0.820	0.978
E	0.0009	6.523	0.901	10.183	0.840	0.976
F	0.0009	6.531	0.972	10.286	0.932	0.922

3.6. Effect of desorption temperature on adsorption-desorption cycle time

Regenerating adsorbents is an important step from economic and environmental viewpoints. The use of adsorbents for the adsorption of certain material should be repeated or prolonged [21]. Desorption is usually conducted by flushing the column with air at various air temperatures, such as ambient temperature ranging from 30 °C to 40 °C. In this experiment, desorption was conducted after the adsorption.

Figure 11 shows the kinetics curves of adsorption and desorption processes. The best temperature for desorption process was 40 °C, where the saturated adsorbent regenerated after 19 minutes. At ambient temperature 30 °C, regeneration took 45 and 40 minutes. Therefore, the higher the desorption temperature, the higher the effectiveness of CO₂ removal from the adsorbent. This result is in accordance with the report by Lee and Lee (2014), who claimed that the higher the desorption temperature, the faster the desorption. Regeneration effectiveness increased due to the increased amount of CO₂ released per unit time [21].

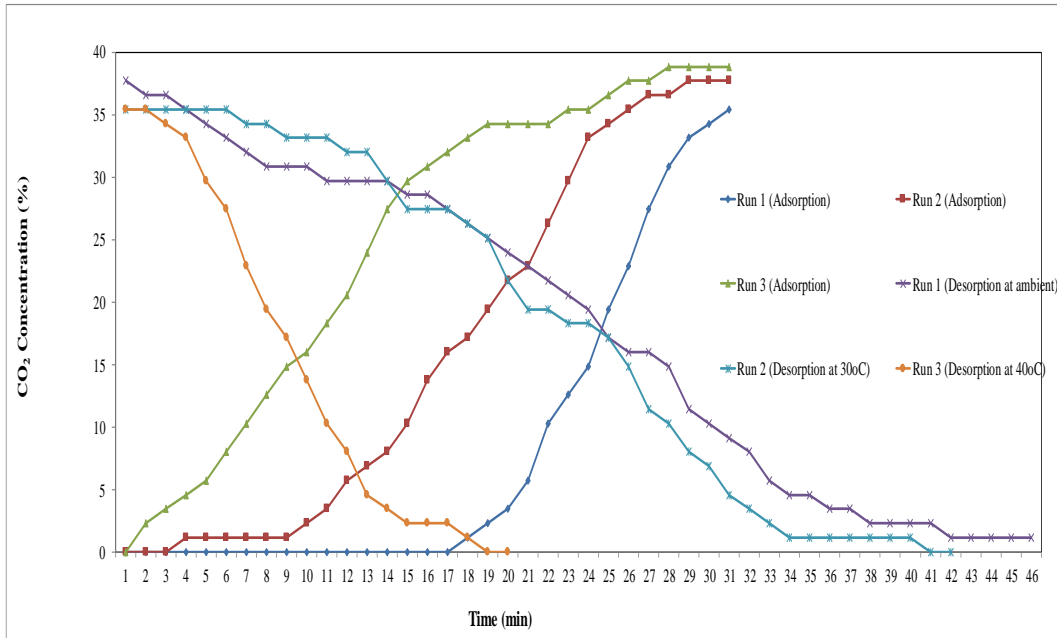


Fig. 11. Effect of desorption temperature on adsorption-desorption cycle time.

4. Conclusions

Low flow rate of mixed gas in the CO₂ removal process increases the retention time of gas in the column because many CO₂ particles are absorbed in the adsorbent than usual. The best type of zeolite pellet used as adsorbent was particle size of 140 mesh and calcination temperature 400 °C for four hours, where the CO₂ removal efficiency reached 92.5% at flow rate of 200 ml/min. The best adsorption capacity was 0.118 mmol/g by using pellet adsorbent with 140 mesh size, calcination temperature 400 °C for 4 hours and flow rate of 400 ml/min with a breakthrough time of 10.7 minutes. The adsorption equilibrium obtained the correlation value $R^2 = 0.9962$ with $q_m = 5.97$ ml/g and $K_L = 9.36$ ml/g. The best kinetic model was pseudo-order kinetics with the best R^2 correlation value = 0.9848 with $q_e = 6.3620$ ml/g and $K_1 = 0.0016$ min⁻¹. The adsorbent could be regenerated after 19 minutes in the desorption using air at 40 °C. Future research must focus on improving the quality of the adsorbent pellets to increase the breakthrough time and reduce the frequency of the adsorption-desorption cycle becomes by conducting chemical-physic activation.

Nomenclatures

C_e	Concentration of adsorbate at equilibrium
K_1	Rate constant of the pseudo-first order, min ⁻¹
K_L	Langmuir equilibrium constant, ml/g
q_e	Amount of adsorbate per mass of adsorbent, ml/g
q_m	Adsorption capacity, ml/g

Greek Symbols

α, β	Elovich constants
-----------------	-------------------

Abbreviations

CPO	Crude palm oil
POM	Palm oil mill
POME	Palm oil mill effluent
PSA	Pressure swing adsorption

References

1. United States Department of Agriculture. (2016). *Oilseeds: world market and trade, foreign agricultural service*. Retrieved January 12, 2017, from <https://www.fas.usda.gov/commodities/oilseeds>.
2. United States Department of Agriculture. (2016). *Indonesia: oilseeds and products annual report*. Retrieved January 12, 2017, from <https://www.fas.usda.gov/data/indonesia-oilseeds-and-products-annual-1>.
3. Trisakti, B.; Irvan; Mahdalena; Taslim; and Turmuzi, M. (2017). Effect of temperature on methanogenesis stage of two-stage anaerobic digestion of palm oil mill effluent (POME) into biogas. *IOP Conference Series: Materials Science and Engineering*, 206, 012027.
4. Madaki, Y.S.; and Seng, L. (2013). Palm oil mill effluent (POME) from Malaysia palm oil mills: Waste or resource. *International Journal of Sciences, Environment and Technology*, 6(2), 1138-1155.
5. Reddy, R. (2016). Value chain of biogas (production, gas upgrading, grid injection and utilization). "SAARC Workshop on Application of On-Grid Biogas Technologies". Kabul, Afghanistan.
6. Alonso-Vicario, A.A.; Ochoa-Gomez, J.R.; Gil-Rio, S.; Aberasturi, O.G.J.; Ramirez-Lopez, C.A.; Torrecilla-Soria, T.; and Dominguez, A. (2010). Purification and upgrading of biogas by pressure swing adsorption on synthetic and natural zeolites. *Microporous and Mesoporous Materials*, 134(1-3), 100-107.
7. Mihic, S. (2004). *Biogas fuel for internal combustion engines*. Annals of the Faculty of Engineering Hunedoara. Tome II, Fascicule 3.
8. Al Mamun, M.R.; Karim, M.R.; Rahman, M.M.; Asiri, A.M.; and Torii, S. (2016). Methane enrichment of biogas by carbon dioxide fixation with calcium hydroxide and activated carbon. *Journal of the Taiwan Institute of Chemical Engineers*, 58, 476-481.
9. Xia, Z.-M.; Li, X.-S.; Chen, Z.-Y.; Li, Gang.; Yan, K.-F.; Xu, C.-G.; Lv, Q.-N.; and Cai, J. (2016). Hydrate-based CO₂ capture and CH₄ purification from

- simulated biogas with synergic additives based on gas solvent. *Applied Energy*, 162, 1153-1159.
10. Titinchi, S.J.J.; Piet, M.; Abbo, H.S.; Bolland, O.; and Schwieger, W. (2014). Chemically modified solid adsorbents for CO₂ capture. *Energy Procedia*, 63, 8153-8160.
 11. Wahono; Krido, S.; Maryana; Roni; Kismurtono, M.; Nisa, K.; and Khoirun (2010). *Modifikasi zeolit lokal gunung kidul sebagai upaya peningkatan performa biogas untuk pembangkit listrik*. UPT Balai Pengembangan Proses dan Teknologi Kimia Lembaga Ilmu Pengetahuan Indonesia, ISSN, 1411-4216.
 12. Wahono, S.K.; and Rizal, W.A. (2014). Biogas filter on local natural zeolite materials. *International Journal of Renewable Energy Development*, 3(1), 1-5.
 13. Yamliha, A.; Argo, B.D.; and Nugroho, W.A.; (2013). Effect of zeolite size during carbon dioxide (CO₂) adsorption in biogas flow. *Jurnal Bioproses Komoditas Tropis*, 1(2), 67-72.
 14. Irvan; Trisakti, B.; Maulina, S.; and Daimon, H. (2018). Production of biogas from palm oil mill effluent: from laboratory scale to pilot scale. *Rasayan Journal of Chemistry*, 11(1), 378-385.
 15. Erhayem, M.; Al-Tohami, F.; Mohamed, R.; and Ahmida, K. (2015). Isotherm kinetic and thermodynamic studies for the sorption of mercury (II) onto activated carbon from *Rosmanirus officinalis* leaves. *American Journal of Analytical Chemistry*, 6(1), 1-10.
 16. Kesnawaty, D.A. (2010). *Capacity testing from adsorption of gas carbon monoxide (CO) using metal oxide and activated carbon*. Thesis. Department of Chemical Engineering, University of Indonesia, Depok.
 17. Dutta, M.; Basu, J.K.; Faraz, M.H.; Gautam, N.; and Kumar, A. (2012). Fixed-bed column study of textile dye direct blue 86 by using a composite adsorbent. *Scholars Research Library*, 4(2), 882-891.
 18. Sathish, S.; and Vivekanandan, S. (2014). Effect of mesophilic and thermophilic temperature on floating drum anaerobic bio-digester. *International Journal of Mechanical and Mechatronics Engineering*, 14(06), 39-43.
 19. Persson, M.; Jonsson, O.; and Wellinger, A. (2006). *Biogas upgrading to vehicle fuel standards and grid injection*. Task 37 - *Energy from Biogas and Landfill Gas*. Report SCG 142, IEA Bioenergy.
 20. Prasetiowati, Y.; and Koestiari, T. (2014). Capacity of adsorption technical bentonite as adsorbent Cd²⁺ ions. *UNESA Journal of Chemistry*, 3(3), 194-200.
 21. Lee, E.J.; and Lee, D.S. (2014). Fabrication of in-needle microextraction device using nichrome wire coated with poly (ethylene glycol) and poly (dimethylsiloxane) for determination of volatile compounds in lavender oils. *Bulletin of Korean Chemical Society*, 35(1), 211-217.
 22. Gueu, S.; Yao, B.; Audoby, K.; and Ado, G. (2007). Kinetics and thermodynamics study of lead adsorption on to activated carbon from coconut and seed hull of the palm tree. *International Journal of Environmental Science and Technology*, 4(1), 11-17.